Effects of Geometric Imperfections on Frequency-Load Interaction of Biaxially Compressed Antisymmetric Angle Ply Rectangular Plates

David Hui
Assistant Professor,
Department of Engineering Mechanics,
The Ohio State University,
Columbus, Ohio 43210
Mem. ASME

The present paper deals with the influence of small geometric imperfections on the vibration frequencies of rectangular, simply supported, angle ply, thin composite plates subjected to inplane uniaxial or biaxial compressive preload. Depending on the amount of preload, the frequencies of laminated plates with different imperfection shapes may be significantly higher than those for perfect plates, especially in a certain range of fiber angles. Interaction curves between frequency and applied preload are plotted for various fiber angles and imperfection amplitudes for both the uniaxial and equal biaxial loading cases.

1 Introduction

Vibration of fiber-reinforced plates and shells has been a subject of significant current interest since it is an important design consideration in many light-weight, high-strength, engineering structural configurations. Based on the pioneering work on the effects of bending-stretching coupling of composite plates by Ambartsumyan [1] and Reissner and Stavsky [2], the vibration frequencies of antisymmetric angle and cross-ply perfect plates with no preload were studied by Whitney and Leissa [3] and subsequently by Jones [4]. Excellent reviews on the current state of the art were written by Chia [5], Leissa [6], and Bert [7].

However, it should be emphasized that none of the foregoing analyses for laminated plates and shells involves the study of the effects of small, usually unavoidable, geometric imperfections (that is, deviation from flatness). Geometric imperfections have been found to be very significant, in some cases, in affecting the linear small-amplitude vibration frequencies of isotropic, homogeneous thin-walled structures such as simply supported rectangular preloaded flat plates [8], externally pressurized shallow spherical shells [9], unstiffened cylindrical shells [10, 11], cylindrical panels [12], and stiffened cylindrical shells [13], even in the absence of inplane compressive preload. Of particular concern is whether the fiber orientation and bending-stretching coupling for laminated plates will significantly affect the sensitivity of the vibration frequencies due to the presence of small geometric imperfections (already found to be significant for homogeneous isotropic flat plates). The effects of a static previbration deformation due to inplane compressive preload will be examined.

If Koiter's work in 1945 on the effects of geometric imperfections on buckling of thin-walled structures is considered a major breakthrough in applied mechanics [14], then the work on establishing the influence of geometric imperfections on vibration of similar structures should also be considered a major breakthrough in the field. Among the existing publications on the possible effects of imperfections on vibrations of plates and shells [8–13], not one of them deals with laminated thin-walled structures. This paper is the first in the open literature to point out that if these laminated structures were actually tested in the laboratory, it is possible that significant increases in the fundamental frequencies may occur due to the presence of unavoidable small geometric imperfections and inplane compressible preload. Further studies on the large-amplitude vibrations of laminated plates will be presented in a separate paper [15].

The present analysis is based on a solution of the nonlinear von Kármán-type governing differential equations within the context of Koiter's special theory of elastic stability [16]. The geometric imperfection is assumed to take the shape of a sinusoidal wave in both of the inplane directions. The static previbration nonlinear compatibility equation is satisfied exactly. Further, the nonlinear previbration static equilibrium equation is satisfied approximately using a Galerkin procedure. Using a perturbation technique, the dynamic equilibrium and compatibility differential equations are

Contributed by the Applied Mechanics Division and presented at the Winter Annual Meeting, New Orleans, La., December 9–14, 1984 of THE AMERICAN SOCIETY OF MECHANICAL ENGINEERS.

Discussion on this paper should be addressed to the Editorial Department, ASME, United Engineering Center, 345 East 47th Street, New York, N.Y. 10017, and will be accepted until two months after final publication of the paper itself in the JOURNAL OF APPLIED MECHANICS. Manuscript received by ASME Applied Mechanics Division, September, 1983; final revision, May, 1984. Paper No. 84-WA/APM-44.

Copies will be available until August, 1985.

linearized with respect to the perturbed dynamic state. The linearized compatibility equation is solved exactly (exact relative to the assumed vibration mode shape) and the dynamic equilibrium equation is then satisfied approximately using a Galerkin procedure. An explicit expression for the vibration frequency is obtained as a function of the biaxial preload, the imperfection amplitude, the vibration wave number, and the imperfection wave numbers.

Example problems are chosen from typical graphite-epoxy angle ply rectangular plates [4, 5, 17] where the optimum fiber angle, taking into account the effects of bending-stretching coupling and imperfection sensitivity, are investigated. Frequency versus uniaxial or equal biaxial load interaction curves are presented for various fiber angles and imperfection amplitudes. It is found that the amplitudes of imperfections on the order of a fraction of the total laminated plate thickness may significantly raise the vibration frequencies, especially in plate configurations corresponding to a certain range of fiber orientations and large uniaxial or biaxial compressive preload.

2 Governing Differential Equations

The von Kármán-type nonlinear equilibrium and compatibility equations for a thin laminated plate (written in terms of a normal displacement W and a stress function F) are, respectively [18, 19],

$$L_{D^*}(W)+L_{B^*}(F)+\rho W,_{\bar{t}\bar{t}}=F,_{YY}(W+W_0),_{XX}+F,_{XX}(W+W_0),_{YY}-2F,_{XY}(W+W_0),_{XY}$$

$$L_{A^*}(F)=L_{B^*}(W)+[(W+W_0),_{XY}]^2-(W_{0,XY})^2-(W+W_0),_{XX}(W+W_0),_{YY}+W_{0,XX}W_{0,YY} \quad (1,2)$$

In the foregoing, $\bar{t}$ is time, ρ is the mass of the plate per unit area, X and Y are the in-plane coordinates, and W_0 is the initial geometric imperfection. The strains and moments are related to the membrane stress resultants and curvatures by ($N_x=F,_{YY}$, $N_y=F,_{XX}$ and $N_{xy}=-F,_{XY}$)

$$[\epsilon_x,\epsilon_y,\gamma_{xy},M_x,M_y,M_{xy}]^T=\begin{bmatrix}[A^*_{ij}] & [B^*_{ij}]\\ -[B^*_{ij}]^T & [D^*_{ij}]\end{bmatrix}\cdot[N_x,N_y,N_{xy},-W,_{XX},-W,_{YY},-2W,_{XY}]^T \quad (3)$$

Introducing the nondimensionalization scheme,

$$(w,w_0)=(W/h,W_0/h),\qquad f=F/(Eh^3),$$

$$(x,y)=(1/b)(X,Y)$$

$$(a^*_{ij},b^*_{ij},d^*_{ij})=(EhA^*_{ij},B^*_{ij}/h,D^*_{ij}/(Eh^3)] \quad (4)$$

where E is an arbitrary Young's modulus, h is the total laminated plate thickness, and b is the width of the plate ($Y=0$ to b). The nonlinear dynamic equilibrium and compatibility equations can be written in nondimensional form,

$$L_{d^*}(w)+L_{b^*}(f)+[\rho b^4/(Eh^3)]w,_{\bar{t}\bar{t}}=f,_{yy}(w+w_0),_{xx}+f,_{xx}(w+w_0),_{yy}-2f,_{xy}(w+w_0),_{xy} \quad (5)$$

$$L_{a^*}(f)=L_{b^*}(w)+[(w+w_0),_{xy}]^2-(w_{0,xy})^2-(w+w_0),_{xx}(w+w_0),_{yy}+w_{0,xx}w_{0,yy} \quad (6)$$

In the special case of angle ply composite plates, the nondimensional linear differential operators are:

$$\begin{aligned}L_{a^*}(\ ) &= a^*_{22}(\ ),_{xxxx}+(2a^*_{12}+a^*_{66})(\ ),_{xxyy}+a^*_{11}(\ ),_{yyyy}\\ L_{b^*}(\ ) &= (2b^*_{26}-b^*_{61})(\ ),_{xxxy}+(2b^*_{16}-b^*_{62})(\ ),_{xyyy}\\ L_{d^*}(\ ) &= d^*_{11}(\ ),_{xxxx}+(2)(d^*_{12}+2d^*_{66})(\ ),_{xxyy}+d^*_{22}(\ ),_{yyyy}\end{aligned} \quad (7)$$

The rectangular angle ply plate is assumed to be simply supported along all four edges ($w=0$ and $M_y=0$ at $y=0$ and $y=1$ and $w=0$, $M_x=0$ at $x=0$ and $x=a/b$ where a is the length of the plate). Further, there is no inplane shear stress along all the edges ($f,_{xy}=0$ on all four edges) and the inplane displacement perpendicular to each edge is constant.

3 Previbration State

The previbration static deformation w_p is assumed to be of the same shape as the initial geometric imperfection ($J=jb/a$ and j and k are positive integers)

$$[w_p(x,y),w_0(x,y)]=(c_w,\mu)\sin(J\pi x)\sin(k\pi y) \quad (8)$$

Substituting $w=w_p(x,y)$ and $w_0(x,y)$ into the nonlinear compatibility equation, the previbration stress function $f_p(x,y)$ which satisfies this nonlinear differential equation exactly is:

$$f_p(x,y)=f^*(x,y)-(\bar{\sigma}_x)(y^2/2)-(\bar{\sigma}_y)(x^2/2) \quad (9)$$

where

$$(\bar{\sigma}_x,\bar{\sigma}_y)=(-N_x,-N_y)(b^2/(Eh^3))$$

and

$$f^*(x,y)=c_f\cos(J\pi x)\cos(k\pi y)+[(c_w+\mu)^2-\mu^2][A_1\cos(2J\pi x)+A_2\cos(2k\pi y)] \quad (10)$$

Further, the constants c_f, A_1, and A_2 are found to be:

$$\begin{aligned}c_f &= (-c_w)C_{b^*}(J,k)/C_{a^*}(J,k)\\ A_1 &= [1/(32a^*_{22})](k/J)^2,\qquad A_2=[1/(32a^*_{11})](J/k)^2\end{aligned} \quad (11)$$

$$\begin{aligned}C_{a^*}(P,Q) &= a^*_{22}P^4+(2a^*_{12}+a^*_{66})(P^2Q^2)+a^*_{11}Q^4\\ C_{b^*}(P,Q) &= (2b^*_{26}-b^*_{61})(P^3Q)+(2b^*_{16}-b^*_{62})(PQ^3)\end{aligned} \quad (12)$$

Substituting $w_p(x,y)$, $w_0(x,y)$, and $f_p(x,y)$ into the nonlinear previbration static equilibrium equation and applying the Galerkin procedure (multiplying both sides by $\sin(J\pi x)\sin(k\pi y)$ and integrating from $x=0$ to a/b and $y=0$ to 1), one obtains a cubic equation in $c_w+\mu$ of the form,

$$(c_w+\mu)^3(2J^2k^2)(A_1+A_2)+(c_w+\mu)\{(-\mu^2)(2J^2k^2)(A_1+A_2)-[(\bar{\sigma}_xJ^2+\bar{\sigma}_yk^2)/\pi^2]+C^*\}-(\mu)C^*=0 \quad (13)$$

where

$$C^*=C_{d^*}(J,k)+C_{b^*}(J,k)^2/C_{a^*}(J,k)] \quad (14)$$

$$C_{d^*}(P,Q)=d^*_{11}P^4+(2)(d^*_{12}+2d^*_{66})(P^2Q^2)+d^*_{22}Q^4 \quad (15)$$

As a check, it can be seen that $\bar{\sigma}_x=\bar{\sigma}_y=0$ implies $c_w=0$. Finally, the applied preloads $\bar{\sigma}_x$ and $\bar{\sigma}_y$ should not be so large as to cause excessive plate deformations. Neglecting the cubic terms in equation (13) (as was done in references [10] and [13]) will result in considerable errors in the previbration deformation for $|\mu|>0.1$.

4 Vibrations of Biaxially Compressed Imperfect Angle Ply Plates

Using a perturbation method, the perturbed dynamic state $w_B(x,y,t)$ and $f_B(x,y,t)$ is added to the previbration state of static equilibrium and the governing differential equations are linearized with respect to $w_B(x,y,t)$ and $f_B(x,y,t)$. Doing so, the dynamic equilibrium and compatibility equations become:

$$L_{d^*}(w_B)+L_{b^*}(f_B)+[\rho b^4/(Eh^3)]w_{B,\bar{t}\bar{t}}+(\bar{\sigma}_xw_{B,xx}+\bar{\sigma}_yw_{B,yy})=f^*,_{yy}w_{B,xx}+f^*,_{xx}w_{B,yy}-2f^*,_{xy}w_{B,xy}+(w_p+w_0),_{xx}f_{B,yy}+(w_p+w_0),_{yy}f_{B,xx}-2(w_p+w_0),_{xy}f_{B,xy} \quad (16)$$

$$L_{a^*}(f_B)=L_{b^*}(w_B)+(2)(w_p+w_0),_{xy}w_{B,xy}-(w_p+w_0),_{xx}w_{B,yy}-(w_p+w_0),_{yy}w_{B,xx} \quad (17)$$

The associated simply supported boundary conditions are $w_B=0$, $w_{B,xx}=0$, and $f_{B,xy}=0$ at $x=0$ and a/b. In anticipation that the two edges $y=0$ and $y=1$ have arbitrary, but uniform, boundary conditions acting along them (e.g.,

clamped, simply supported, or free), including the case when they are reinforced by stringers that may provide torsional restraint on the plate (the actual nonclassical boundary condition may lie somewhere between the simple support and clamped boundary conditions so that a discretized numerical solution is necessary [17]). It is desirable to reduce the dynamic equilibrium and compatibility equations to ordinary differential equations in the y direction.

The vibration mode is assumed to be of the form,

$$w_B(x,y,t) = \sin(M\pi x) w_B(y) \exp(i\omega \bar{t}) \tag{18}$$

where ω is the vibration frequency, $M = mb/a$, and m is the number of half sin-waves from $x=0$ to $x=a/b$. Substituting $w_B(x,y,t)$, $w_p(x,y)$, and $w_0(x,y)$ into the foregoing linearized compatibility equation, one obtains three coupled ordinary differential equations in the form,

$$\begin{aligned} &a_{22}^*(M\pi)^4 f_1(y) + (2a_{12}^* + a_{66}^*)(-M^2\pi^2) f_1(y)_{,yy} \\ &\quad + a_{11}^* f_1(y)_{,yyyy} = (2b_{26}^* - b_{61}^*)(-M^3\pi^3) w_B(y)_{,y} \\ &\quad + (2b_{16}^* - b_{62}^*)(M\pi) w_B(y)_{,yyy} \end{aligned} \tag{19}$$

$$\begin{aligned} &a_{22}^*(J-M)^4\pi^4 f_2(y) + (2a_{12}^* + a_{66}^*)(-\pi^2) \\ &\quad (J-M)^2 f_2(y)_{,yy} + a_{11}^* f_2(y)_{,yyyy} \\ &= (1/2)(c_w+\mu)[(2MJK\pi^3) w_B(y)_{,y} \cos(k\pi y) \\ &\quad + (J^2\pi^2) w_B(y)_{,yy} \sin(k\pi y) \\ &\quad - (M^2k^2\pi^4) w_B(y) \sin(k\pi y) \end{aligned} \tag{20}$$

$$\begin{aligned} &a_{22}^*(J+M)^4\pi^4 f_3(y) + (2a_{12}^* + a_{66}^*)(-\pi^2) \\ &\quad (J+M)^2 f_3(y)_{,yy} + a_{11}^* f_3(y)_{,yyyy} \\ &= (1/2)(c_w+\mu)[(2MJk\pi^3) w_B(y)_{,y} \cos(k\pi y) \\ &\quad - (J^2\pi^2) w_B(y)_{,yy} \sin(k\pi y) \\ &\quad + (M^2k^2\pi^4) w_B(y) \sin(k\pi y) \end{aligned} \tag{21}$$

where the stress function $f_B(x,y,t)$ is:

$$\begin{aligned} f_B(x,y,t) = \{&f_1(y)\cos(M\pi x) + f_2(y)\cos[\\ &(J-M)\pi x] + f_3(y)\cos[(J+M)\pi x]\} \exp(i\omega \bar{t}) \end{aligned} \tag{22}$$

Substituting $w_B(x,y,t)$, $f_B(x,y,t)$, $w_p(x,y)$, $w_0(x,y)$, and $f^*(x,y)$ into the linearized dynamic equilibrium equation and applying the Galerkin procedure (multiply both sides by $\sin(M\pi x)$ and integrating from $x=0$ to $x=a/b$), one obtains an ordinary differential equation involving $f_1(y)$, $f_2(y)$, $f_3(y)$, and $w_B(y)$ in the form:

$$\begin{aligned} &(1/2)\{[d_{11}^* M^4\pi^4 - \pi^4\Omega^2 - (M\pi)^2\bar{\sigma}_x] w_B(y) \\ &\quad + [\bar{\sigma}_y - 2(d_{12}^* + 2d_{66}^*)(M\pi)^2] w_B(y)_{,yy} \\ &\quad + d_{22}^* w_B(y)_{,yyyy} + (2b_{26}^* - b_{61}^*)(M\pi)^3 f_1(y)_{,y} \\ &\quad + (2b_{16}^* - b_{62}^*)(-M\pi) f_1(y)_{,yyy} \\ &\quad + 2(I_0)[(2b_{26}^* - b_{61}^*)(J-M)^3\pi^3 f_2(y)_{,y} \\ &\quad + (2b_{16}^* - b_{62}^*)(-\pi)(J-M) f_2(y)_{,yyy}\} \\ &= [(c_w+\mu)^2 - \mu^2]\{(2M^2k^2\pi^4 A_2) w_B(y)\cos(2k\pi y) \\ &\quad - (4J^2\pi^2 A_1)(I_1) w_B(y)_{,yy}\} \\ &\quad + (M^2k^2\pi^4 c_f)(I_2) w_B(y)\cos(k\pi y) \\ &\quad - (J^2\pi^2 c_f)(I_2) w_B(y)_{,yy}\cos(k\pi y) \\ &\quad - (2JkM\pi^3 c_f)(I_3) w_B(y)_{,y}\sin(k\pi y) \\ &\quad + (c_w+\mu)\sin(k\pi y)\{-I_3 J^2\pi^2 f_1(y)_{,yy} \\ &\quad + k^2M^2(I_3\pi^4) f_1(y) + (-J^2\pi^2 I_4) f_2(y)_{,yy} \\ &\quad + \pi^4 k^2 (J-M)^2 I_4 f_2(y) + (-J^2\pi^2 I_5) f_3(y)_{,yy} \\ &\quad + \pi^4 k^2 (J+M)^2 I_5 f_3(y)\} \\ &\quad + (c_w+\mu)\cos(k\pi y)\{(2JkM\pi^3) I_2 f_1(y)_{,y} \\ &\quad + (2Jk)(J-M)\pi^3 I_6 f_2(y)_{,y} \\ &\quad + (2Jk)(J+M)\pi^3 I_7 f_3(y)_{,y}\} \end{aligned} \tag{23}$$

In the preceding expression, $\pi^4\Omega^2 = \omega^2\rho b^4/(Eh^3)$ and $E = E_2$ where E_2 is Young's modulus in the plane of the plate, perpendicular to the fiber direction, and the definite integrals I_0, $I_1, \ldots, I_7$ are defined in the Appendix. Equations (19)–(21) and (23) constitute four coupled ordinary differential equations in four unknowns variables $f_1(y)$, $f_2(y)$, $f_3(y)$, and $w_B(y)$. The appropriate (possibly nonclassical) boundary conditions at $y=0$ and $y=1$ can be formulated in a manner similar to the one presented in reference [17]. The differential equations and boundary conditions may then be solved exactly, which involves considerable work, or they may be discretized and solved numerically.

Since the objective of the present paper is to examine the effects of the geometric imperfections on the vibrations of axially compressed angle ply plates in a relatively straightforward manner, the boundary conditions at the edges $y=0$ and $y=1$ are taken to be simply supported so that $w_B = 0$, $w_{B,yy} = 0$ and $f_{B,xy} = 0$. Thus, one may assume:

$$w_B(y) = \xi \sin(n\pi y) \tag{24}$$

where n is the number of half sine-waves from $y=0$ to $y=1$ and ξ is the amplitude of vibration mode normalized with respect to the laminated plate thickness. Substituting $w_B(y)$ into equations (16)–(18), one obtains:

$$\begin{aligned} f_1(y) &= \xi c_1 \cos(n\pi y) \\ f_2(y) &= \xi(c_w+\mu)\{c_2\cos[(k-n)\pi y] + c_3\cos[(k+n)\pi y]\} \\ f_3(y) &= \xi(c_w+\mu)\{c_4\cos[(k-n)\pi y] + c_5\cos[(k+n)\pi y]\} \end{aligned} \tag{25}$$

where ($c_2 = 0$ if $Jn = kM$),

$$\begin{aligned} c_1 &= -C_b^*(M,n)/C_a^*(M,n) \\ c_2 &= (-1)(Jn-kM)^2/[4C_a^*(J-M,k-n), \\ c_3 &= (Jn+kM)^2/[4C_a^*(J-M,k+n)] \\ c_4 &= (Jn+kM)^2/[4C_a^*(J+M,k-n)], \\ c_5 &= (-1)(Jn-kM)^2/[4C_a^*(J+M,k+n)] \end{aligned} \tag{26}$$

It may be verified that the preceding analysis is valid for the two special cases when $n = k/2$ and $n = k$.

Finally, substituting $f_1(y)$, $f_2(y)$, $f_3(y)$, and $w_B(y)$ into the linearized dynamic equilibrium equation (23) and again applying the Galerkin procedure (multiplying both sides by $\sin(n\pi y)$ and then integrating from $y=0$ to $y=1$), one obtains an explicit expression involving the frequency squared and the applied inplane biaxial loads $\bar{\sigma}_x$ and $\bar{\sigma}_y$ in the form:

$$\begin{aligned} &\Omega^2 + [(M^2\bar{\sigma}_x + n^2\bar{\sigma}_y)/\pi^2] = C_d^*(M,n) \\ &\quad + [C_b^*(M,n)^2/C_a^*(M,n)] \\ &\quad - (4I_0H_0c_2)(c_w+\mu)C_b^*(J-M,k-n) \\ &\quad - [(c_w+\mu)^2 - \mu^2][(8M^2k^2)(A_2H_1) \\ &\quad + (8J^2n^2)(A_1I_1)] - (4c_fI_2H_2)(M^2k^2 + J^2n^2) \\ &\quad + (8JkMn)(c_fI_3H_3) \\ &\quad - (4c_1)(c_w+\mu)(J^2n^2 + k^2M^2)(H_3I_3) \\ &\quad + (8JkMn)(c_w+\mu)(I_2H_2c_1) \\ &\quad - (4)(c_w+\mu)^2\{[J^2(k-n)^2 + k^2(J-M)^2](c_2I_4H_4) \\ &\quad + [J^2(k+n)^2 + k^2(J-M)^2](c_3I_4H_5) + [J^2(k-n)^2 \\ &\quad + k^2(J+M)^2](c_4I_5H_4) + [J^2(k+n)^2 \\ &\quad + k^2(J+M)^2](c_5I_5H_5)\} \\ &\quad + (8Jk)(c_w+\mu)\{(J-M)[c_2(k-n)(I_6H_6) \\ &\quad + c_3(k+n)(I_6H_7)] + (J+M)[c_4(k-n)(I_7H_6) \\ &\quad + c_5(k+n)(I_7H_7)]\} \end{aligned} \tag{27}$$

The definite integrals H_0, $H_1, \ldots, H_7$ are defined in the Appendix. As a check on the analysis, when both the frequency Ω and the imperfection amplitude μ are set equal to zero, the foregoing equation agrees with the buckling load

expression obtained by Harris [20]. The buckling load for a perfect ($\mu = 0$) rectangular angle ply plate is ($n = 1$ if $\bar{\sigma}_y = 0$),

$$\bar{\sigma}_x + \bar{\sigma}_y = (\pi^2)\{C_d^*(M,n) + [C_b^*(M,n)^2/C_a^*(M,n)]\} \quad (28)$$

5 Results and Discussion

Due to the large number of parameters involved, it is not practical to present a complete study on the effects of parameter variations. Thus, example problems are selected from typical graphite-epoxy angle ply laminated rectangular plates [4, 5, 17] with (E is chosen to be E_2)

$$E_1/E_2 = 40, \quad G_{12}/E_2 = 0.5, \quad \nu_{12} = 0.25, \quad \nu_{21} = \nu_{12}(E_2/E_1) \quad (29)$$

where E_1 and E_2 are inplane Young's moduli parallel and perpendicular to the filament direction, respectively, ν_{12} and ν_{21} are Poisson's ratios, and G_{12} is the shear modulus. The aspect ratio a/b is chosen to be unity and simple support boundary conditions at the four edges are enforced. Furthermore, to investigate the effects of bending-stretching coupling, laminated plates with even number of equal-thickness layers N being $N = 2$ and $N =$ infinite are considered. The angle ply plates are subjected to the possibility of two inplane compressive stresses and the initial geometric imperfections are taken to be sine waves in both the inplane x and y directions ($J = k = 1$; $J = k = 2$; $J = 1, K = 2$; $J = 2, k = 1$ for no preload and $J = k = 1$ for preload).

In the present example problem of square angle-ply plates with uniaxial preload in the x direction, the optimum value of the wave number n in the y direction that renders the frequency a minimum (that is, the fundamental mode) is found to be 1. For equal biaxial preload (that is, hydrostatic inplane compression), the optimum value of axial wave number m is found to be 1 for $\theta \leq 45$ deg while the optimum value of n in the y direction is 1 for $\theta \geq 45$ deg (θ is the fiber angle measured from the axial x direction). The optimum wave numbers are found to be $m = n = 1$ in both the uniaxial and equal biaxial preload cases provided the preload is sufficiently small or zero.

Figure 1(a) shows a graph of normalized fundamental frequency $\omega/\omega(\theta = \mu = 0)$ versus normalized uniaxial preload $\bar{\sigma}_x/\bar{\sigma}_{x_c}(\theta = \mu = 0)$. The fundamental frequency and the classical buckling load at $\theta = 0$ and $\mu = 0$ are, respectively,

$$\pi^2\Omega(\theta = \mu = 0) = [\rho b^4/(Eh^3)]^{1/2}\omega(\theta = \mu = 0) = 18.805$$

$$\bar{\sigma}_{x_c}(\theta = \mu = 0) = 35.8307 \quad (30)$$

Geometric imperfection amplitudes of 0, ± 0.5, and ± 1.0 are used for fiber angles of 0 deg and 90 deg. It can be seen that imperfections may significantly raise the frequencies due to initial curvature effects. For sufficiently small values of the uniaxial preload $\bar{\sigma}_x$, the 0 deg and 90 deg curves coincide for a fixed value of the imperfection amplitude. However, for larger amount of uniaxial preload, there is a significant decrease in the fundamental frequencies for the 90 deg curves due to the influence of vibrational modes with higher axial wave numbers. These higher modes do not correspond to lower fundamental frequencies for the 0 deg curves because the laminated plate for the 0 deg fiber angle is much stiffer against bending in the axial x direction than those for the 90 deg fiber angle. For design purposes, taking into account the possibility of the presence of geometric imperfections in the order of the laminated plate thickness, it can be seen that the 0 deg configuration is stiffer than the 90 deg orientation both in terms of vibration with uniaxial preload and buckling (note that buckling occurs when $\Omega = 0$). Clearly, the number of layers N will not affect either the 0 deg or 90 deg configurations.

Figure 1(b) shows a graph of normalized frequency versus normalized uniaxial preload for $\theta = 15$ deg with various values of imperfection amplitude and for the number of layers N being 2 and infinite ($N = 4$ curve is shown only for $\mu = 0$). Again, the presence of geometric imperfections may result in a significant increase in the vibration frequencies. The optimum value of the axial wave number m is found to be 1 for all these curves. A larger rate of increase of the frequency (μ is fixed) due to uniaxial preload is found for $N = 2$ (where the effects of bending-stretching coupling is most pronounced) than for $N =$ infinity (which corresponds to the orthotropic plate).

Figure 1(c) is a plot of normalized frequency versus normalized uniaxial preload for $\theta = 75$ deg with values of imperfection amplitude being 0, ± 0.5, and ± 1.0 for $N = 2$ and infinity. For a fixed value of the imperfection amplitude and for a sufficiently small amount of uniaxial preload, these curves for the 75 deg configuration coincide with those for the 15 deg orientation presented in Fig. 1(b). However, for larger uniaxial preload, the presence of higher modes with larger values of m is found to significantly reduce the vibration frequencies. The optimum axial wave numbers m are shown in the figure.

Similarly, Fig. 1(d) shows curves for $\theta = 45$ deg. Although the degrading effects of bending-stretching coupling ($N = 2$) in the vibration frequency for sufficiently small amount of uniaxial preload is quite pronounced, these curves rise quite rapidly for larger amount of uniaxial preload. Judging from all the preceding figures, it may be observed that the buckling loads ($\omega = 0$) are not reduced due to the presence of initial geometric imperfections ($J = k = 1$).

Summarizing Figs. 1(a)–(d), it may be said that for any given inplane uniaxial preload, an increase in imperfection amplitude causes increase in the fundamental frequency. This is due to two factors: (a) the slight initial curvature due to imperfection increases the stiffness, and (b) uniaxial preload causes additional curvature.

Figures 2(a)–(c) present results for the case of equal biaxial stress ($\bar{\sigma}_x = \bar{\sigma}_y$) showing the effects of preload on the fundamental frequency for various values of imperfection amplitude μ being 0, ± 0.5, and ± 1.0. The previously used values of $\omega(\theta = \mu = 0)$ and $\bar{\sigma}_{x_c}(\theta = \mu = 0)$ are again used as normalizing factors. Figure 2(a) shows curves for the case of 0 deg and 90 deg orientations. Unlike the case of 0 deg orientation for the uniaxial preload as shown in Fig. 1(a), none of the curves for lowest wave numbers (m = n = 1) is applicable for very large equal biaxial preload (that is, all the curves eventually drop) due to the dominance of vibration modes with higher wave numbers. The optimum wave number m is always 1 and the optimum value of n is shown in the figure for the 0 deg orientation. Due to symmetry consideration for square plates in equal biaxial loading, the curves for the 90 deg orientation are identical to that for the 0 deg configuration (for a fixed value of the imperfection amplitude) provided that the optimum values for m and n are interchanged. The number of layers do not affect the 0 deg nor the 90 deg configurations.

Figure 2(b) gives data in the cases of 15 deg and 75 deg configurations. Due to symmetry, unlike the uniaxial preload case ($\bar{\sigma}_y = 0$) of Figs. 1(b) and (c), the 15 deg and 75 deg curves coincide even for large values of the equal biaxial preload. Again, small imperfections are shown to have a pronounced effect on raising the vibration frequencies. In general, care should be taken not to apply excessively large inplane compressive preload (say twice the buckling load) in order to avoid numerical inaccuracies in the previbration deformations.

For brevity, the plot for $\theta = 45$ deg will not be presented. For $\theta = 45$ deg, the optimum wave numbers are found to be $m = n = 1$ for $a/b = 1$ in all these curves. Again, the presence of small imperfections may significantly raise the vibration frequencies. It should be noted that these curves are identical to that presented in Fig. 1(d) for uniaxial preload ($\bar{\sigma}_y = 0$) except that the compressive preload axis is shrunk by a factor

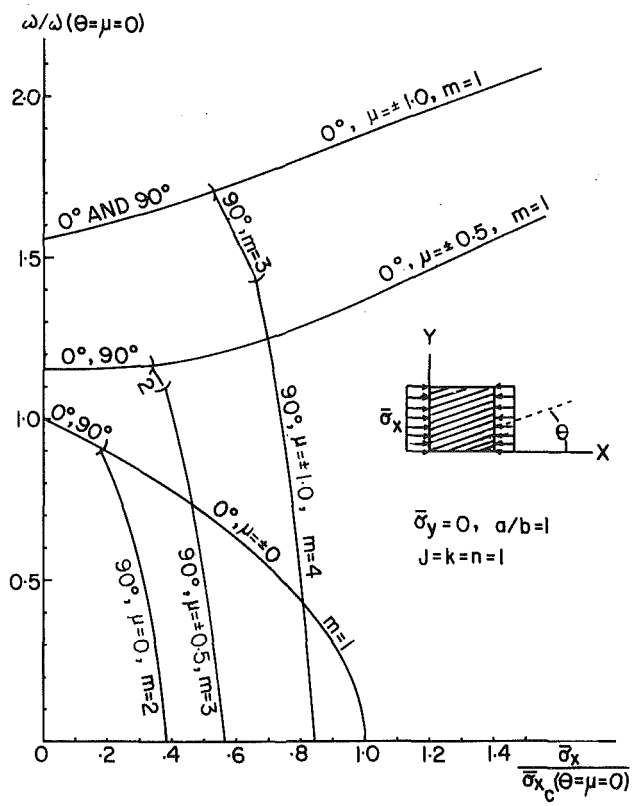

Fig. 1(*a*) Normalized fundamental frequency versus normalized uniaxial preload for imperfect angle ply plates ($\theta = 0$ deg and 90 deg, $J = k = 1$)

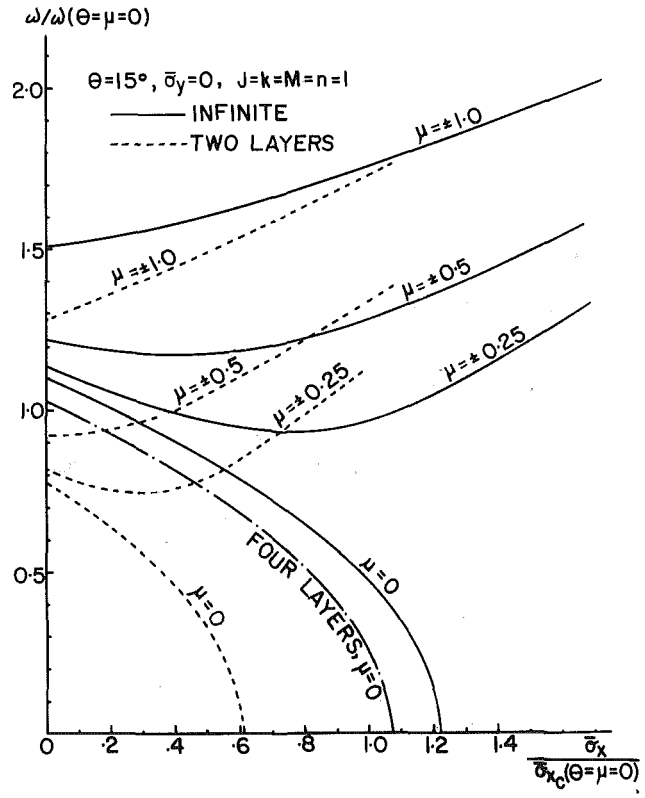

Fig. 1(*b*) Normalized fundamental frequency versus normalized uniaxial preload for imperfect angle ply plates ($\theta = 15$ deg, $J = k = 1$)

of 2. Thus, the frequency increase due to imperfections becomes more important for a given value of preload in the equal biaxial case.

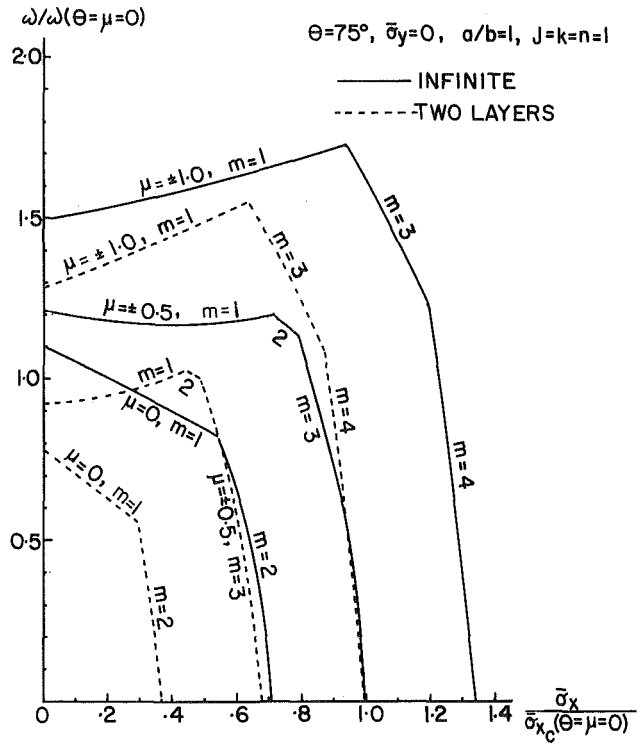

Fig. 1(*c*) Normalized fundamental frequency versus normalized uniaxial preload for imperfect angle ply plates ($\theta = 75$ deg, $J = k = 1$)

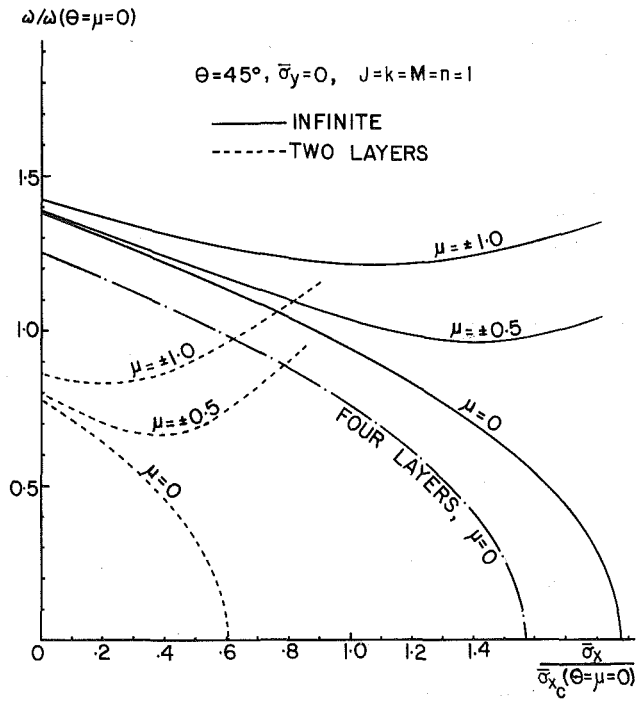

Fig. 1(*d*) Normalized fundamental frequency versus normalized uniaxial preload for imperfect angle ply plates ($\theta = 45$ deg, $J = k = 1$)

Fig. 1

Figure (3*a*) depicts normalized frequency versus fiber angle θ for simply supported square angle ply laminated plates with various values of imperfection amplitudes and imperfection wave numbers ($\mu = 0$, ± 0.5, and ± 1.0 for $J = k = 1$ and $\mu = 0$ and ± 1.0 for $J = k = 2$) and number of layers ($N = 2$ and $N =$ infinity), in the important special case of no inplane

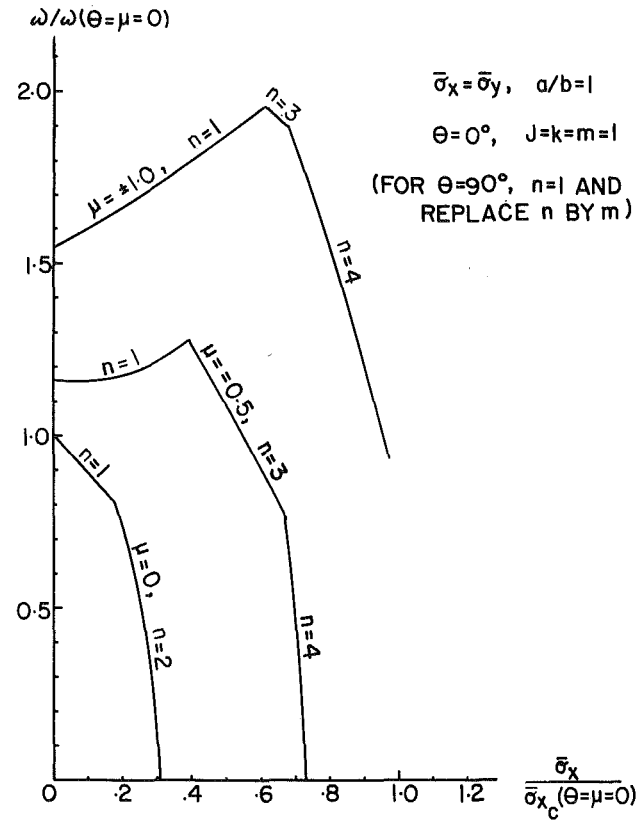

Fig. 2(a) Normalized fundamental frequency versus normalized equal biaxial preload for imperfect angle ply plates ($\theta = 0$ deg and 90 deg, $J = k = 1$)

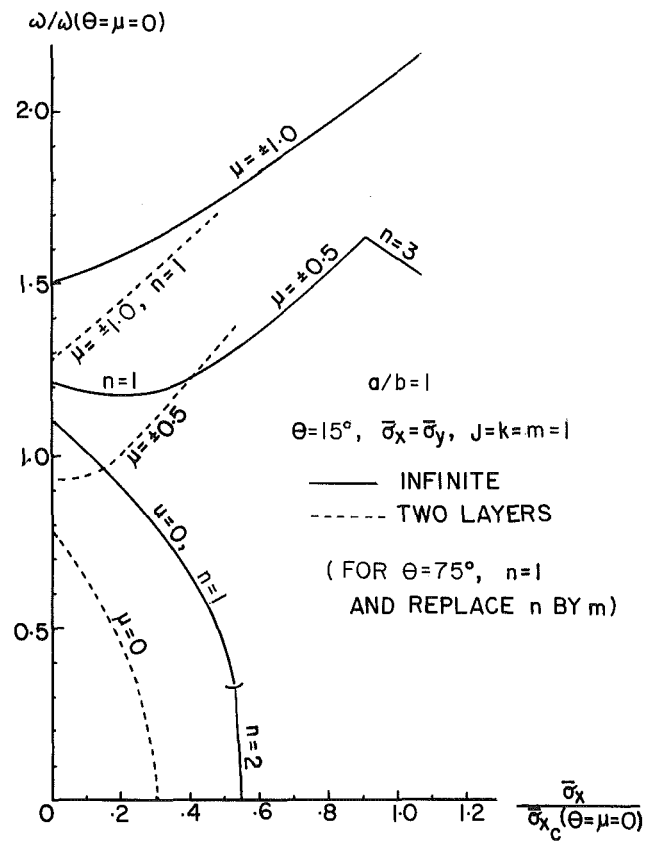

Fig. 2(b) Normalized fundamental frequency versus normalized equal biaxial preload for imperfect angle ply plates ($\theta = 15$ deg and 75 deg, $J = k = 1$)

Fig. 2

preload. Due to symmetry, the curves for the θ and 90 deg-θ configurations coincide. For orthotropic plates (N = infinity) with imperfection wave numbers $J = k = 1$, it can be seen that the effects of geometric imperfection on raising the fundamental frequencies are more pronounced for fiber orientations approximately parallel to the edges ($\theta \approx 0$ deg and 90 deg) than for the diagonal orientations ($\theta \approx 45$ deg). The same conclusion is also applicable to two-layer plates with $J = k = 1$. On the other hand, the effects of imperfections of the type $J = k = 2$ on raising the fundamental frequencies are more pronounced for fiber orientations θ between 15 deg and 30 deg than for the remaining range of θ, both in the case of N = infinity and $N = 2$. The reduction of the frequencies due to the bending-stretching coupling effects can be seen by comparing the N = infinity and $N = 2$ curves.

Finally, the normalized frequency versus fiber angle θ for the other two types of geometric imperfections ($\theta = 0, \pm 1.0$ for $J = 1$, $k = 2$ and $J = 2$, $k = 1$) are presented in Fig. 3(*b*). For a given number of layers, the effects of geometric imperfections of the type $J = 1$, $k = 2$ in raising the fundamental frequencies are more pronounced in the 0 deg $\leq \theta \leq$ 25 deg range than in the 25 deg $< \theta \leq 45$ deg range. On the other hand, the increases in fundamental frequencies due to the $J = 2$, $k = 1$ type of geometric imperfections are more pronounced in the 20 deg $< \theta <$ 35 deg than in the 0 deg $\leq \theta \leq$ 25 deg and 35 deg $\leq \theta \leq 45$ deg ranges. Due to symmetry, the curves for the θ configuration with $J = 1$, $k = 2$ are identical to those for the 90 deg-θ configuration with $J = 2$, $k = 1$. As a check, all the curves in Figs. 3(*a*) and (*b*) have zero slope at $\theta = 0$ deg and $\theta = 45$ deg. These curves agree with the plotted values in Figs. 1(*a*)-(*d*) and 2(*a*)-(*c*) in the special case of no preload ($J = k = 1$).

6 Concluding Remarks

The effects of geometric imperfections on vibrations of simply supported angle-ply plates in the cases of uniaxial or equal biaxial preload are analyzed. It is found that significant increases in the fundamental frequencies typically occur for geometric imperfection amplitudes of the order of the laminated plate thickness. In the case of uniaxial preload, the increase of frequency due to the geometric imperfection of the type $J = k = 1$ is much more pronounced for smaller fiber angles (e.g., $\theta = 0$ deg and $\theta = 15$ deg) than for larger angles (e.g., $\theta = 75$ deg and 90 deg) due to the fact that the vibration modes with larger axial wave numbers m correspond to higher (i.e., nonfundamental) frequencies for small fiber angles. For equal biaxial preload, the similar effects of geometric imperfections ($J = k = 1$) in raising the fundamental frequencies are again detected. The vibration modes with larger wave numbers may correspond to the lowest (i.e., fundamental) frequencies for both large and small fiber angles, but not at or near the $\theta = 45$ deg configurations. The influence of various types of geometric imperfections ($J = k = 1$, $J = k = 2$, $J = 1, k = 2$, and $J = 2, k = 1$) on the fundamental frequencies for all fiber angles with no preload have been examined. Extensions of this work to laminated cylindrical panels and laminated cylindrical shells are in progress.

Acknowledgment

This research was supported by the Ohio State research seed grant awarded to the author through the Office of Research and Graduate Studies.

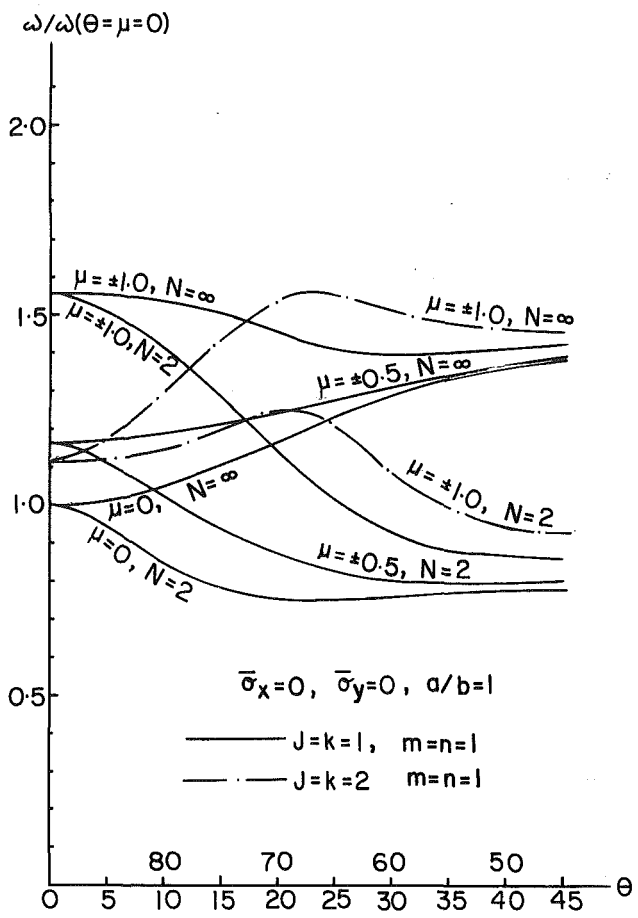

Fig. 3(*a*) Normalized fundamental frequency versus fiber angle with imperfection wave numbers $J = k = 1$ and $J = k = 2$ (no preload)

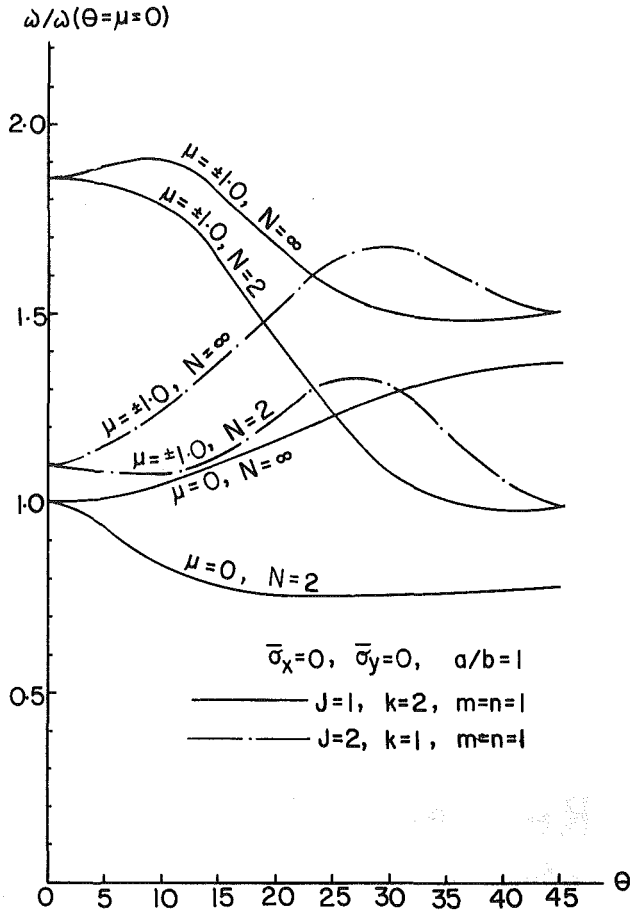

Fig. 3(*b*) Normalized fundamental frequency versus fiber angle with imperection wave numbers $J = 1, k = 2$ and $J = 2, k = 1$ (no preload)

Fig. 3

References

1 Ambartsumyan, S. A., "Calculation of Laminated Anisotropic Shells," *Izvestiia Akademiia Nauk Armenskoi SSR, Ser. Fiz. Mat. Est. Tekh. Nauk.*, Vol. 6, No. 3, 1953, p. 15.

2 Reissner, E., and Stavsky, Y., "Bending and Stretching of Certain Types of Heterogeneous Aeolotropic Elastic Plates," ASME JOURNAL OF APPLIED MECHANICS, Vol. 28, 1961, pp. 402–408.

3 Whitney, J. M., and Leissa, A. W., "Analysis of Heterogeneous Anisotropic Plates," ASME JOURNAL OF APPLIED MECHANICS, Vol. 36, 1969, pp. 261–266.

4 Jones, R. M., *Mechanics of Composite Materials*, Scripta, 1975.

5 Chia, C. Y., *Nonlinear Analysis of Plates*, McGraw-Hill, New York, 1980, 430 pp.

6 Leissa, A. W., "Advances in Vibration, Buckling and Postbuckling Studies on Composite Plates," *Composite Structures, Proc. of 1st Int. Conf. Sept. 1981*, Marshall, I. H., ed., Applied Science, 1981, pp. 312–334.

7 Bert, C. W., "Research on Dynamics of Composite and Sandwich Plates, 1979–1981," *The Shock and Vibration Digest*, Vol. 14, No. 10, Oct. 1982, pp. 17–34.

8 Hui, D., and Leissa, A. W., "Effects of Geometric Imperfections on Vibrations of Biaxially Compressed Rectangular Flat Plates," ASME JOURNAL OF APPLIED MECHANICS, Vol. 50, No. 4, 1983, pp. 750–756.

9 Hui, D., and Leissa, A. W., "Effects of Uni-Directional Geometric Imperfections on Vibrations of Pressurized Shallow Spherical Shells," *International Journal of Nonlinear Mechanics*, Vol. 18, No. 4, 1983, pp. 279–285.

10 Rosen, A., and Singer, J., "Influence of Asymmetric Imperfections on the Vibrations of Axially Compressed Cylindrical Shells," *Israel J. of Technology*, Vol. 14, 1976, pp. 23–26; also Technion Aeronautical Engineering, TAE Report No. 212, Mar. 1975.

11 Watawala, L., and Nash, W. A., "Influence of Initial Geometric Imperfections on Vibrations of Thin Circular Cylindrical Shells," *Computers and Structures*, Vol. 16, Nos. 1–4, 1983, pp. 125–230.

12 Hui, D., "Effects of Geometric Imperfections and In-Plane Constraints on Nonlinear Vibrations of Simply Supported Cylindrical Panels," ASME JOURNAL OF APPLIED MECHANICS, Vol. 51, No. 2, 1984, pp. 383–390.

13 Singer, J., and Prucz, J., "Influence of Initial Geometrical Imperfections on Vibrations of Axially Compressed Stiffened Cylindrical Shells," *J. of Sound and Vibration*, Vol. 80, No. 1, 1982, pp. 117–143; also Technion Aeronautical Engineering TAE Report No. 369, Feb. 1980, 113 pp.

14 Budiansky, B., and Hutchinson, J. W., "Buckling: Progress and Challenge," *Proceedings of Symposium on Trends in Solid Mechanics*, 1979, Delft University Press, The Netherlands.

15 Hui, D., "Soft-Spring Nonlinear Vibrations of Antisymmetrically Laminated Rectangular Plates," submitted to *Proc. of 5th ASCE-EM Specialty Conference*, University of Wyoming, Aug. 1–3, 1984, pp. 372–375.

16 Koiter, W. T., "The Effect of Axisymmetric Imperfection on the Buckling of Cylindrical Shells Under Axial Compression," *Koninklijke Nederlandse Academie Wetenschappen*, Proc. Series *B.*, Vol. 66, 1963, pp. 265–279.

17 Hui, D., and Hansen, J. S., "Effect of Stringer Torsional Rigidity on Buckling of Integrally Stiffened Angle Ply Plates," *Fibre Science and Technology Journal*, Vol. 16, Jan. 1982, pp. 39–43.

18 Stavsky, Y., and Hoff, N. J., "Mechanics of Composite Structures," *Composite Engineering Laminates*, Dietz, A.G.H., ed MIT Press, Cambridge, Mass., and London, England, 1969, pp. 5–59.

19 Tennyson, R. C., Muggeridge, D. B., Chan, K. H., and Khot, N. S., "Buckling of Fiber-Reinforced Circular Cylinders under Axial Compression," AFFDL-TR-72-102, Aug. 1972, 114 pp.

20 Harris, G. Z., "The Buckling and Post-Buckling Behavior of Composite Plates Under Biaxial Loading," *Int. J. of Mechanical Sciences*, Vol. 17, 1975, pp. 187–202.

APPENDIX

Definite Integrals

The functions $I(\ )$ and $H(\ )$ are defined to be,

$$I(\ ) = (b/a)\int_0^{a/b} (\ )dx, \qquad H(\ ) = \int_0^1 (\ )dy \quad (A1\text{–}A2)$$

and the definite integrals $I_0, I_1, I_2, \ldots, I_7$ are,

$$I_0 = I[\sin(M\pi x)\sin[(J-M)\pi x]] = 1/2 \quad \text{if} \quad 2M=J; \quad 0 \quad \text{otherwise}$$

$$I_1 = I[\sin^2(M\pi x)\cos(2J\pi x)] = -1/4 \quad \text{if} \quad M=J; \quad 0 \quad \text{otherwise}$$

$$I_2 = I[\sin^2(M\pi x)\cos(J\pi x)] = -1/4 \quad \text{if} \quad 2M=J; \quad 0 \quad \text{otherwise}$$

$$I_3 = I[\sin(M\pi x)\cos(M\pi x)\sin(J\pi x)] = 1/4 \quad \text{if} \quad 2M=J; \quad 0 \quad \text{otherwise}$$

$$I_4 = I[\sin(M\pi x)\sin(J\pi x)\cos[(J-M)\pi x]] = 1/2 \quad \text{if} \quad M=J; \quad 0 \quad \text{otherwise}$$

$$I_5 = I[\sin(M\pi x)\sin(J\pi x)\cos[(J+M)\pi x]] = -1/4$$

$$I_6 = I[\sin(M\pi x)\cos(J\pi x)\sin[(J-M)\pi x]] = -1/4 \quad \text{if} \quad 2M=J; \quad 0 \quad \text{otherwise}$$

$$I_7 = I[\sin(M\pi x)\cos(J\pi x)\sin[(J+M)\pi x]] = 1/4 \qquad (A3\text{–}A10)$$

The definite integrals H_i is defined to be I_i (where $i=0, 1, 2, \ldots 7$) by replacing J and M by k and n, respectively. For example,

$$H_0 = H[\sin(n\pi y)\sin[(k-n)\pi y]] = 1/2 \quad \text{if} \quad 2n=k; \quad 0 \quad \text{otherwise}$$

$$H_1 = H[\sin^2(n\pi y)\cos(2k\pi y)] = -1/4 \quad \text{if} \quad n=k; \quad 0 \quad \text{otherwise} \qquad (A11\text{–}A12)$$

It can be easily verified that $H_0=I_0, H_1=I_1, H_2=I_2, H_3=I_3, H_4=I_4, H_5=I_5, H_6=I_6$ and $H_7=I_7$ provided the foregoing substitutions are carried out.